An investigation into the preparation of rare earth metals by carbothermic reduction in tin

by

Lee Samuel Lyons, Jr.

A Thesis Submitted to the
Graduate Faculty in Partial Fulfillment of the
Requirements for the Degree of
MASTER OF SCIENCE

Major: Metallurgy

Iowa State University
Ames, Iowa

1980

TABLE OF CONTENTS

ABSTRACT

The reduction of Nd_2O_3 and Gd_2O_3 by C in a Sn solvent was investigated over the temperature range 1585-1760°C and a vacuum of 10^{-5} torr. Reduction of Nd_2O_3 by C was accomplished by heating at 1700°C for 17 hours under a vacuum of 10^{-5} torr. Nd-Sn alloys prepared in this manner contained 0.7% C and 0.06% O. The reduction of Gd_2O_3 by C in a Sn solvent was accomplished by heating at 1760°C for 17 hours under a vacuum of 10^{-5} torr. The Gd-Sn alloys prepared under these conditions contained ∿1.8% C and 0.3% O. Because of the higher reaction temperature (>1760°C) Gd-Sn alloys contained more carbon than Nd-Sn alloys. It was thought that the higher carbon contents were from the graphite crucibles used to contain the Gd-Sn alloys.

All efforts to vacuum distill Sn from Nd-Sn and Gd-Sn alloys were unsuccessful. In the case of Nd-Sn alloys, vacuum distillation at ∿1760°C for 3 hours resulted in the formation of a phase with the approximate composition Nd_5Sn_3. Vacuum distillation of Gd-Sn alloys at 1760-1800°C for 4.5 hours resulted in the formation of a black magnetic and nonmetallic powder with the composition 42.3 a/o Sn and 57.7 a/o Gd. Thus, our investigations showed that carbothermic reduction of Nd_2O_3 and Gd_2O_3 in a Sn solvent, and subsequent vaporization of Sn, cannot be used to prepare pure Nd and Gd metals. Neither was the intermediate Nd-Sn and Gd-Sn alloys particularly pure, especially with respect to C and O.

I. INTRODUCTION

A. Review of Methods Used to Prepare Rare Earths

The preparation of rare earth metals has been done successfully by the following methods:

1. metallothermic reduction of the fluoride,
2. metallothermic reduction of the oxide,
3. metallothermic reduction of the chloride,
4. and electrowinning of the chloride, fluoride and oxide.

A fifth method, carbothermic reduction of the oxide, has been used to prepare Sc and some of the volatile rare earths.[1] However, this method has not been adopted to a commercial scale. Each of the four above methods have been recently reviewed by Beaudry and Gschneidner.[2] Consequently, only the fundamental aspects of each method will be considered here.

1. Metallothermic reduction of the fluoride

The preparation of rare earth metals via metallothermic reduction of the fluorides begins with the pure oxides. Using pure starting materials significantly reduce the amount of impurities in the final metal product. The rare earth oxides prepared in the Ames Laboratory for this study were 99.999% pure with respect to all rare earth impurities and other cation impurity elements. Volatile impurities are not of much concern because they can be removed by vacuum melting the rare earth metals.

Metallothermic reduction of the rare earth fluorides can be divided into three groups depending upon the procedure used to prepare them. The melting and boiling points determine what metals belong to what group.

Group I consists of La, Ce, Pr and Nd which have low melting points and high boiling points. Y, Gd, Tb and Lu which have moderate to high melting points and high boiling points make up Group II. The elements Sc, Dy, Ho and Er which have high melting points and moderate boiling points compose Group III. The remaining natural occurring rare earths, Sm, Eu, Tm and Yb, have low boiling points and are obtained by direct reduction from their respective oxides rather than their respective fluorides.

The conversion of the rare earth oxides to the fluorides is accomplished by the two step process of Spedding and Henderson as described in reference 2. Essentially, the process consists of passing anhydrous HF and 60% Ar over the rare earth oxide at 700°C for 16 hours. The oxide is contained in a Pt boat to prevent contamination of the oxides and the fluoride product. The second step consists of heating the fluoride approximately 50° above its melting point in a Pt crucible under a dynamic HF:60% Ar atmosphere. This is done to quantitatively convert the remaining oxide to fluoride.

In all cases, the reductant metal is triply distilled Ca metal. The Ca reductant must be handled in an inert atmosphere because of its chemically reactive nature that can lead to further contamination of the final product.

The reaction crucibles are constructed of "high purity, pickled and annealed Ta sheet". These crucibles are heated in a vacuum of 1×10^{-6} torr to 1900°C to remove volatile impurities.

A typical reduction of fluorides from Group I can be illustrated as follows: fifteen per cent excess Ca of the theoretical amount required to reduce the fluoride is mixed with CeF_3 and packed in a Ta crucible in a He-filled glove box. The reaction crucible is placed in a vacuum

induction furnace and the pressure is reduced to 1×10^{-6} torr. Ar is admitted to the system and the crucible and reactants heated to a temperature above the melting point of the highest melting reactant or product. After reacting the CaF_2 slag floats to the top of the metal. The Ca, CaF_2 and H are removed by vacuum melting.

The metals in Groups II and III are prepared by a variation of the above method. However, after vacuum melting they are further purified, primarily to remove the dissolved Ta, by distillation. In addition, the distillation conditions are different for the two groups.

2. Metallothermic reduction of the oxide

Because of their high vapor pressures, the rare earth metals Sm, Eu, Tm and Yb are prepared by the reaction

$$2La + R_2O_3 \rightarrow La_2O_3 + 2R \uparrow \qquad (1)$$

in which the reaction goes to completion due to removal of these metals by volatilization. Mischmetal* may be used to reduce Sm, Eu and Yb from their oxides if the cost of La is important.(2) However, if mischmetal is used to prepare Tm it will be contaminated with Nd from the mischmetal. Thus, La or Ce must be used for the reduction of Tm if high purity is required.

---

*Mischmetal is an alloy which contains the rare earth metals in the same proportions as found in the original ore sources from which the mischmetal was made. Mischmetal prepared from Bastnasite contains 33% La, 50% Ce, 4% Pr, 12% Nd and 1% Y plus the remaining lanthanides; while that prepared from monazite contains 21% La, 47% Ce, 6% Pr, 20% Nd, 2% Gd, 2% Y and 2% the remaining lanthanides.

3. Metallothermic reduction of the chloride

Rare earth metals have been prepared by Li reduction of the chlorides. Y was the first of the rare earths produced by this process. Reduction of the rare earth chlorides by Li has been adapted to a commercial scale.[2] Essentially, the process consisted of placing crude chloride and commercial grade Li into the apparatus shown in Figure 1. The chamber was evacuated and heated to distill the RCl_3 into the lower crucible shown. After reaction, a molten mixture of rare earth and LiCl slag was obtained. The LiCl slag was distilled from the reaction curcible. The low melting rare earth metals were consolidated by arc melting or induction melting. Because of the low reaction temperature (800-1000°C), the resulting rare earth metals were not contaminated with crucible material. A variation of this method has been used by Carlson and Schmidt to obtain high purity Y.[2]

4. Electrowinning of the chloride, fluoride and oxide

Presently, the electrolytic method is used to prepare the largest amounts of rare earth metals.[2] The electrolytic method is the cheapest of all methods used to prepare rare earths. However, there are severe limitations to the electrolytic process, the most serious one being the limited 1100°C operating temperature because of the reactivity of the rare earths at elevated temperatures. Therefore, this method is limited to the first four lanthanide metals, La, Ce, Pr, Nd and mischmetal.

La, Ce, Pr, Nd and mischmetal are prepared commercially by electrowinning from their chlorides. The chlorides are hygroscopic and difficult

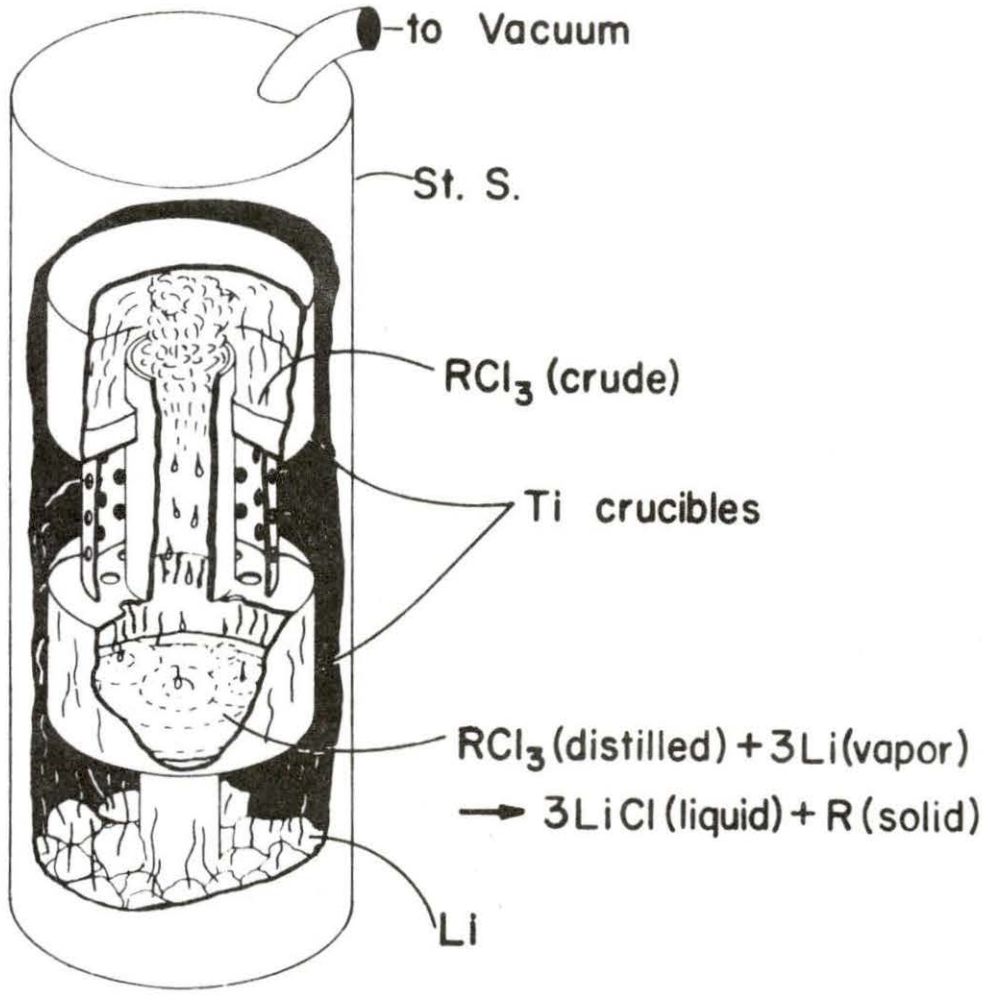

Figure 1. Reduction crucible used for the Li reduction of RCl_3

to handle. Therefore, high purity La, Ce, Pr and Nd are obtained by electrodeposition from the fluorides because they are not hygroscopic.

The electrolytic reduction of the oxides of La, Ce, Pr and Nd has been done successfully. This method has not been successfully applied to the preparation of the other rare earths owing to their high melting points. However, recent studies by Gschneidner and co-workers have shown that high purity Gd metal can be obtained by electrowinning at $\sim 900^{\circ}C$ and collecting solid Gd dendrites at the cathode.[2, 3, 4, 5] In addition to electrowinning, Zwilling and Gschneidner have also reported the electrorefining of Gd in a molten fluoride electrolyte.[6]

B. Carbothermic Reduction of the Oxide

Carbothermic reduction of reactive metal oxides has been used to produce metals that do not form stable carbides. For example, the F. J. Hansgrig process has been used to obtain Mg by the reduction of MgO with carbon.

$$MgO_{(s)} + C_{(s)} \overset{2200^{\circ}K}{\rightarrow} Mg_{(g)} + CO_{(g)} \uparrow \qquad (2)$$

The reaction is possible because Mg vaporizes as it forms. In addition, the evolution of CO gas drives the reaction to the right. However, reaction (2) can undergo reversion unless precautions are taken to separate the Mg and CO vapors.

The extraction of Zn by carbothermic reduction of ZnO has been adapted to a commercial scale.

$$ZnO_{(s)} + C_{(s)} \rightarrow Zn_{(g)} + CO_{(g)} \uparrow \qquad (3)$$

Reaction (3) will also exhibit reversion if the reduced metal is not

removed as it forms. In spite of this drawback, good quality Mg and Zn can be prepared by carbothermic reduction of the respective oxides.

Carbothermic reduction of Al_2O_3 has been attempted for a number of years, but with little success. Reduction of Al_2O_3 by carbon takes place to some extent at temperatures approaching 2000°C. However, the predominant product is a complicated mixture of carbide and oxy-carbide.

The carbothermic reduction of uranium oxides has been studied for at least two hundred years. The earliest known attempts to reduce uranium oxides with carbon were done by Klaprath in 1789 as described in reference 7. It was a hundred years after the discovery of U that Moissan showed that carbothermic reduction could be used to prepare U metal. The uranium metal, however, was highly contaminated with carbon.

Interests were renewed in the carbothermic reduction of uranium oxide during World War II. The Sylvania process resulted from these efforts, and was used to prepare 100-pound quantities of the metal. Even this process suffered from low yields and carbon contamination. This work was further improved by Wilhelm in 1960, but again the U metal obtained was contaminated with carbon.[7]

The preparation of rare earths by carbothermic reduction has received some attention as indicated by a number of patent claims and other literature on the subject. Probably the most complete work in this area was done by the French worker Achard and the Soviet worker Kystobaeva.[8, 9] A patent has also been granted for the preparation of volatile rare earths by carbothermic reduction.[1] Esstentially, the process of heating a charge of rare earth oxides mixed with carbon under high vacuum (10^{-8} torr) and high temperatures, >1900°C. The intermediate products

are the rare earth carbides. The carbides are thermally decomposed to the metals. It has been reported that Sm, Nd, Eu, Dy, Ho, Er and Tm can be prepared by this method. However, no known commercial process for preparing rare earths is based on this method. Thus, to date there has been no commercial process that allows direct carbothermic reduction of rare earth oxides, and for that matter, most other active metal oxides, to the metal without carbide formation.

II. THEORY OF CARBOTHERMIC REDUCTION

A. Generalized Equations for Carbothermic Reduction

The generalized reaction for carbothermic reduction can be written as follows[7]:

$$MO_z + (x + y)C = M + xCO_2 + yCO \quad (4)$$

where $z = (2x + y)$. The basis for any carbothermic reduction of a metal oxide is the Boudouard reaction

$$2CO_{(g)} = C_{(s)} + CO_{2(g)}. \quad (5)$$

It is a combination of the following reactions:

$$C_{(s)} + \tfrac{1}{2} O_{2(g)} = CO_{(g)} \quad (6)$$

$$C_{(s)} + O_{2(g)} = CO_{2(g)} \quad (7)$$

Using Figure 2, it can be seen that at 1 atm total pressure the standard free energy for the oxidation of carbon to CO and the standard free energy of formation for CO_2 are equal at 710°C. At temperatures below 710°C, CO is a more active reducing agent, and at temperatures above 710°C solid carbon is the more active reducing agent. Thus, the oxidation of carbon will produce a mixture of CO and CO_2, but at low temperatures CO_2 will be the predominant gas phase in equilibrium with graphite, whereas at high temperatures (>710°C) CO is the predominant gaseous component.

It has been shown that at 710°C and 1 atm total pressure the free energy difference between reactions (6) and (7) is zero. Therefore, reducing the pressure shifts reaction (5) to the left in accordance with Le Chatelier's Principle. The significance of this statement and reaction (5) will be elaborated in later sections.

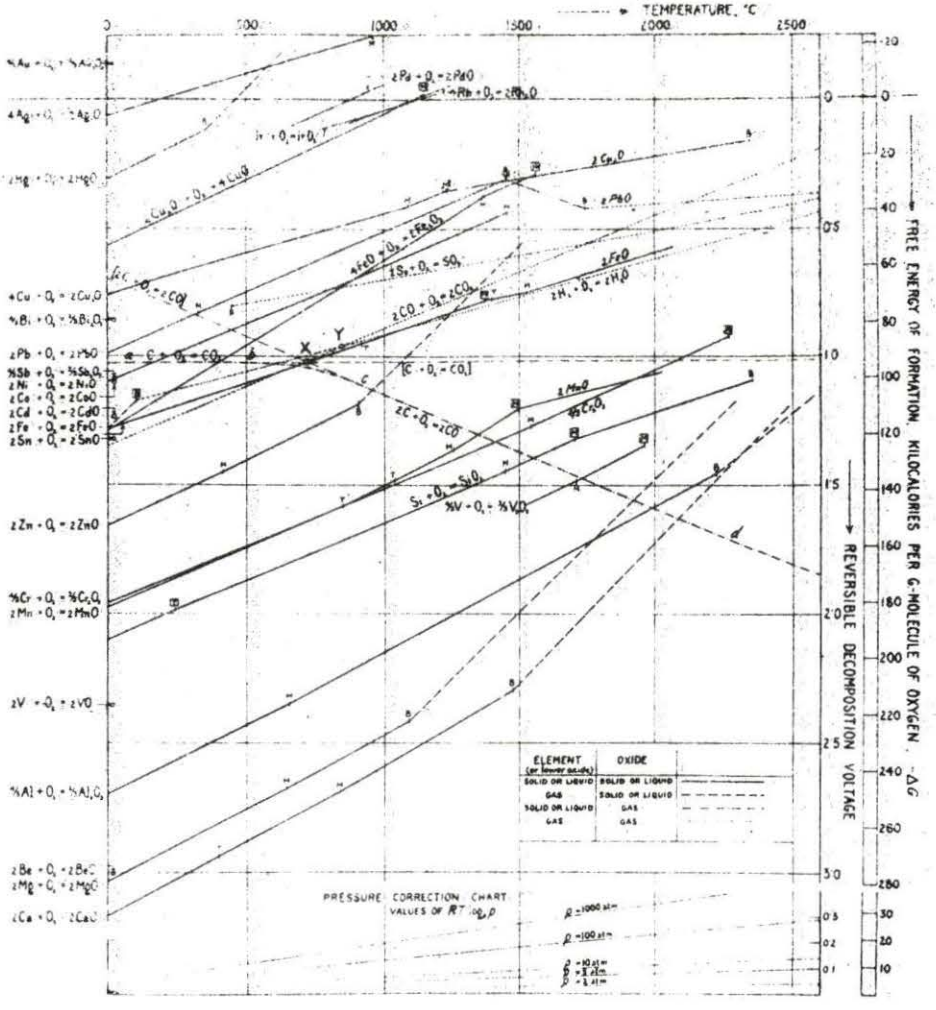

Figure 2. The Ellingham diagram for metallurgically important oxides

B. Problems Associated with Carbothermic Reduction

Carbothermic reduction of rare earth oxides and other reactive metal oxides poses two formidable problems:

1. formation of stable carbides, and
2. the use of temperatures >2000°C.

Firstly, the formation of carbides during reduction is often undesirable. The carbides usually do not have much commercial value, with the exception of uranium, tungsten, etc., and are better avoided. In general, the desired product is the metal and not the carbide.

The formation of carbides during carbothermic reduction follows directly from thermodynamic considerations. Reaction (4) can proceed to an appreciable extent, but carbide formation will intervene if the free energy of the reaction is less negative than the free energy for the formation of carbides, i.e., the following reaction:

$$M + xC \rightarrow MCx. \qquad (8)$$

Unfortunately, this is the case for the reduction of most active metal oxides with carbon. Thus, the problem of carbide formation must be solved before there is hope of carrying out a successful carbothermic reduction.

Secondly, the reduction of most active metal oxides with carbon requires high temperatures. The necessity of using high temperatures can be visualized by examining a plot of free energy of formation of oxides versus temperature, see Figures 2 and 3. For example, consider the carbothermic reduction of Al_2O_3 at 1 atm total pressure:

$$Al_2O_3 + 3C \rightarrow 3CO\uparrow + 2Al. \qquad (9)$$

It can be seen from Figure 2 that the lines for the formation of Al_2O_3

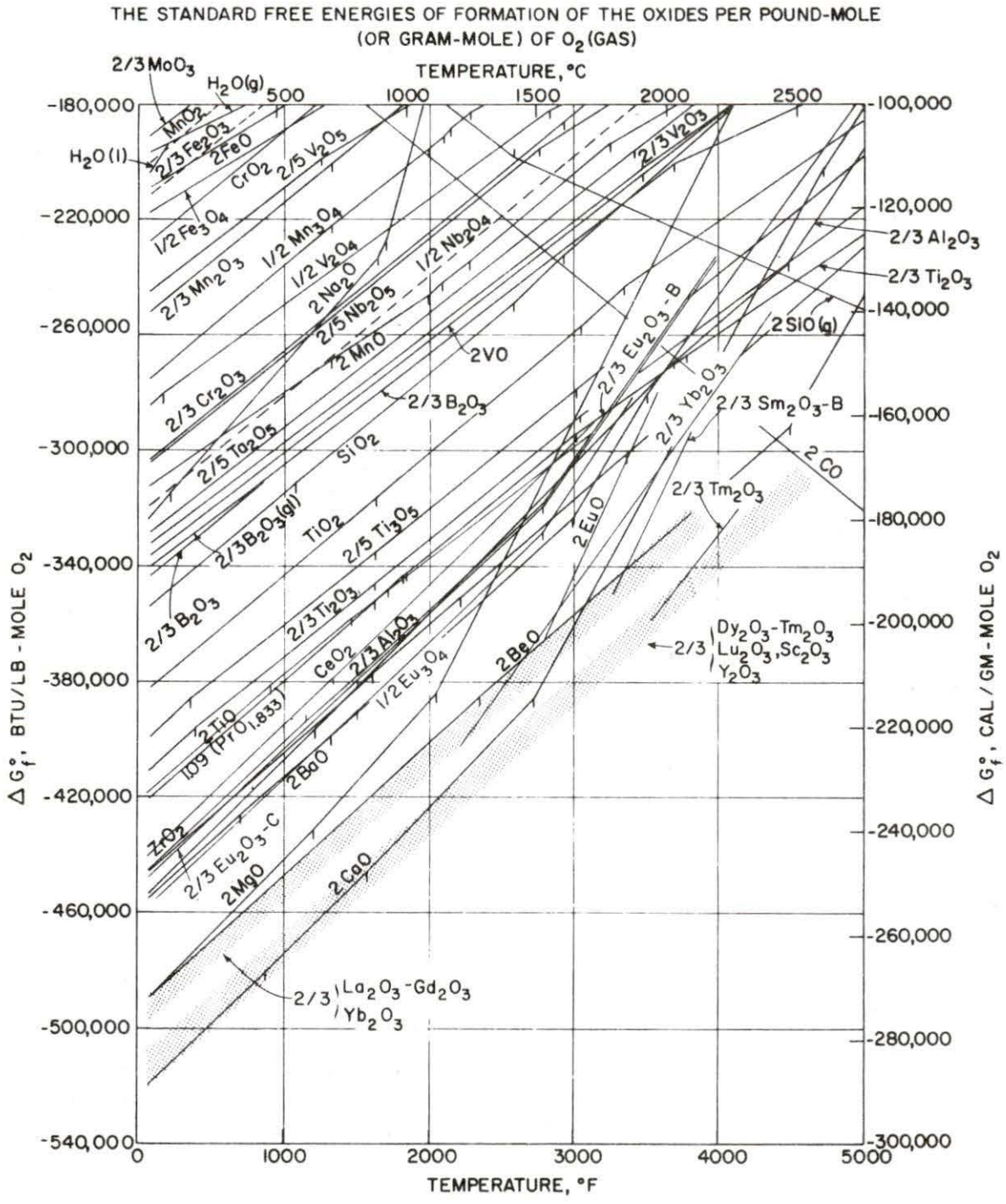

Figure 3. Free energy of formation of oxides

and CO cross at a temperature of 2000°C. At this temperature and 1 atm pressure, the free energy change for reaction (9) is zero. This can be interpreted to mean that the reduction of Al_2O_3 by carbon will start at 2000°C and 1 atm total pressure. At temperatures below 2000°C and 1 atm total pressure, no reduction by carbon is possible because the ΔG for reaction (9) is positive, whereas above 2000°C the free energy for the reaction becomes negative.

C. Overcoming the Problems of Carbothermic Reduction

In order to more fully understand the effects of pressure on the position of the line generated by equation (5), consider the following reaction:

$$2CO + O_2 = 2CO_2. \tag{10}$$

Equation (10) results because at any temperature T, the CO/CO_2 mixture in equilibrium with solid carbon exerts an equilibrium oxygen pressure by way of (10). If solid carbon is to be used as a reducing agent for the oxide MO_2 at the temperature T, then the $pO_2(eq)$ for (10) must be less than the $pO_2(eq)$ for the reaction

$$M + O_2 = MO_2. \tag{11}$$

The Ellingham line for reaction (11) is shown in Figure 4. The line for reaction (11) is seen to intersect the line cs at the temperature T_s, which is the temperature at which ΔG for the reaction

$$MO_2 + 2CO = M + 2CO_2 \tag{12}$$

is zero, i.e.,

$$\Delta G^{\circ}_{(11)} \text{ at } T_s = 0 = -RT \ln \frac{P_{CO_2}{}^2}{P_{CO}{}^2}. \tag{13}$$

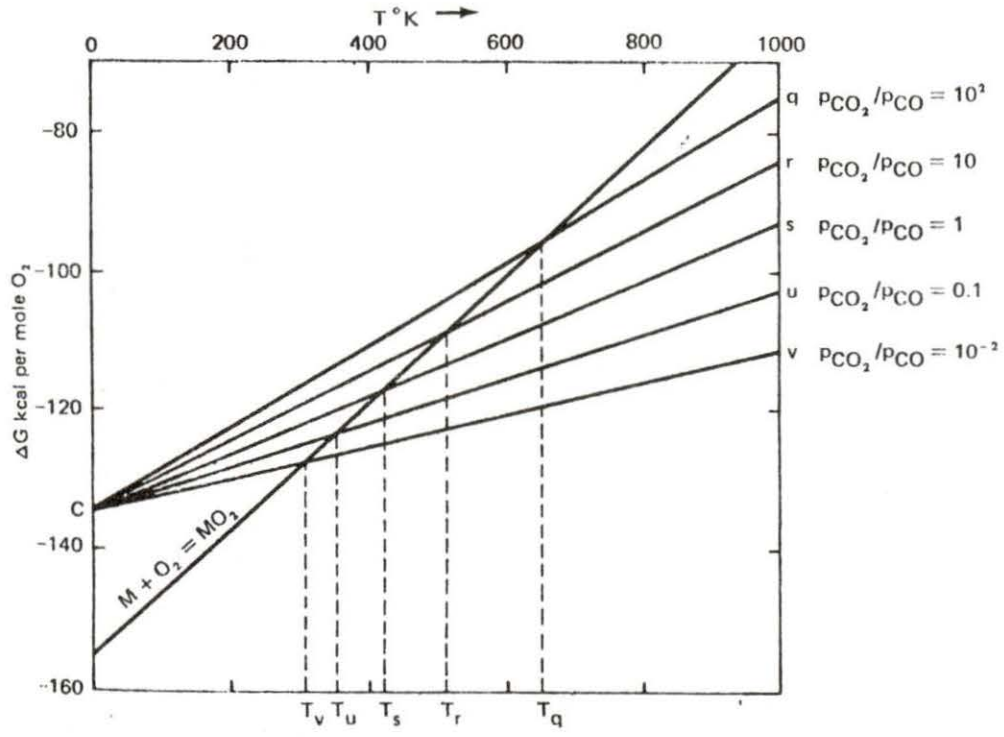

Figure 4. Illustration of the effect of the pCO_2/pCO ratio in a CO-CO_2 gas mixture on the temperature at which the reaction equilibrium $M + CO_2 = MO + CO$ is established.

At temperatures above T_s a $CO-CO_2$ mixture of $P_{CO}/P_{CO_2} = 1$ is reducing with respect to MO_2, and oxidizing with respect to metal temperatures below T_s. Decreasing the P_{CO_2}/P_{CO} ratio shifts the line generated by equation (5) so that it will intersect the line for reaction (2) at lower temperatures. Therefore, the temperatures for reduction of a metal oxide can be lowered by decreasing P_{CO_2}/P_{CO} ratio by use of a vacuum.

Earlier, it was stated that the problem of carbide formation frequently hampers carbothermic reduction of active metal oxides. Turning once more to thermodynamics, one can solve the problem of carbide formation by alloying with elements that are not themselves carbide formers. Alloying reduces the chemical activity of the reduced metal to a level so that carbide formation is prevented. The use of Sn as an alloying element in the carbothermic reduction of UO_2 has been studied by Anderson and Parlee.[10] In this study it was claimed that reduction of UO_2 by carbon in Sn was accomplished over a temperature range of 1550° to $1630^{\circ}C$ and 1 to 10 torr CO. The U metal obtained after evaporation of the Sn was claimed to contain only 0.0008% C, 0.0015% O and 5% Sn. In addition, success was also claimed for the carbothermic reduction of Si, Zr, Ti, Al and Mg using Sn as the solvent. Also it was suggested that this process could be used to prepare rare earth metals.[11] Thus, the purpose of this study was to show that the rare earth metals Nd and Gd could be produced by carbothermic reduction of Nd_2O_3 and Gd_2O_3 in Sn.

The alloying element chosen for this study was Sn. Tin was chosen because:

1. it forms stable intermetallic compounds with Nd and Gd, and
2. it has a high boiling point.

Firstly, one of the criteria established by Anderson et al. for the solvent approach to carbothermic reduction was that the solvent must form stable intermetallic compounds with the reduced metal.[10] The solvent metal decreases carbide formation by lowering the chemical activity of the reduce metal. The known compounds of Sn-Nd and Sn-Gd are $NdSn_3$, Nd_5Sn_3, Nd_5Sn_4, $GdSn_3$, Gd_2Sn_3, and Gd_5Sn_3. Some thermodynamic data for the RSn_3 compounds is given in Table 1.

Table 1. Thermodynamic data for the intermetallic compounds $NdSn_3$ and $GdSn_3$

Compound	ΔG_T (Kcal/mole)	ΔH_T (Kcal/mole)	ΔS_T (e.u.)	(^oK)	Ref.
$NdSn_3$	-49.5[a]	-62.1 ± 0.8	-12.9 ± 0.9	973	12
$GdSn_3$	-42.4 ± 0.2	-53.2 ± 2.0	-10.3 ± 0.2	973	12

[a]Calculated from $\Delta G = \Delta H - T\Delta S$

Secondly, a solvent metal was needed with a high boiling for the carbothermic reduction of Nd_2O_3 and Gd_2O_3. Figure 3 shows that in order to reduce Nd_2O_3 and Gd_2O_3 with carbon under one atmosphere total pressure the reaction temperature would be in excess of 2000^oC. Obviously, not many metals that meet the criterion for solvents can be used under these conditions. The solvent metal would simply distill off before the reduction was complete. Therefore, one must choose a solvent that has a high boiling point. Based on its chemical and physical properties, Sn was chosen because it best matched the conditions for carbothermic reduction, Table 2.

Table 2. Vapor pressure data for selected elements[a]

Element	Vapor pressure (atm)	Temperature (°C)
Sn	10^{-8}	927
	10^{-6}	1127
	10^{-2}	1824
	1	2603
Nd	10^{-8}	955
	10^{-6}	1175
	10^{-2}	2029
	1	3068
Gd	10^{-8}	1167
	10^{-6}	1408
	10^{-2}	2306
	1	3266

[a]See reference 13 for source

III. EXPERIMENTAL

A. Equipment Used for Carbothermic Reduction

The major equipment used in this study consisted of a graphite resistance furnace, fore pump, oil diffusion pump, graphite crucibles, an optical pyrometer, and a catalytic converter. A photograph of the graphite resistance furnace and crucible is given in Figure 5. The maximum temperature obtainable for this particular design of furnace was about 1900°C. Temperature measurements were made using a calibrated optical pyrometer. Essentially, the calibration procedure consisted of placing an empty graphite crucible in the hot zone of the furnace and evacuating the system to 5×10^{-6} torr. The power was turned on and the temperature measured with an optical pyrometer by sighting on the bottom of the crucible through a hole in the crucible lid. The resulting temperatures were plotted as a function of voltage, Figure 6. A block diagram of the reduction system is given in Figure 7.

A catalytic converter was used to convert the evolved carbon monoxide to carbon dioxide. The catalyst was composed of 60% MnO_2 and 40% CuO. The resulting gases were vented to a fume hood.

The pumping capacity of the oil diffusion pump was about 5×10^{-7} torr when the heater was off and 1×10^{-5} torr when on. Pressure variations were followed using an ionization vacuum gauge.

B. Materials Used for Carbothermic Reduction

The rare earth oxides used in this study were obtained from the Ames Laboratory in the form of 99.999% pure powders. Graphite in the form

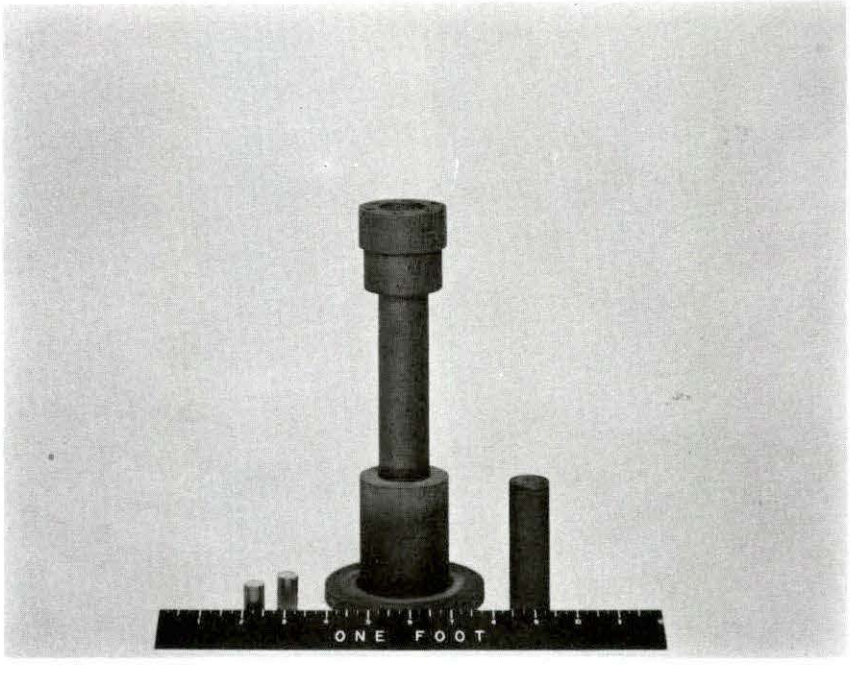

Figure 5. Materials used in carbothermic reduction of rare earth oxides. From left to right, pelletized reactants (C, Sn and R_2O_3), graphite resistance heater and graphite crucible with lid.

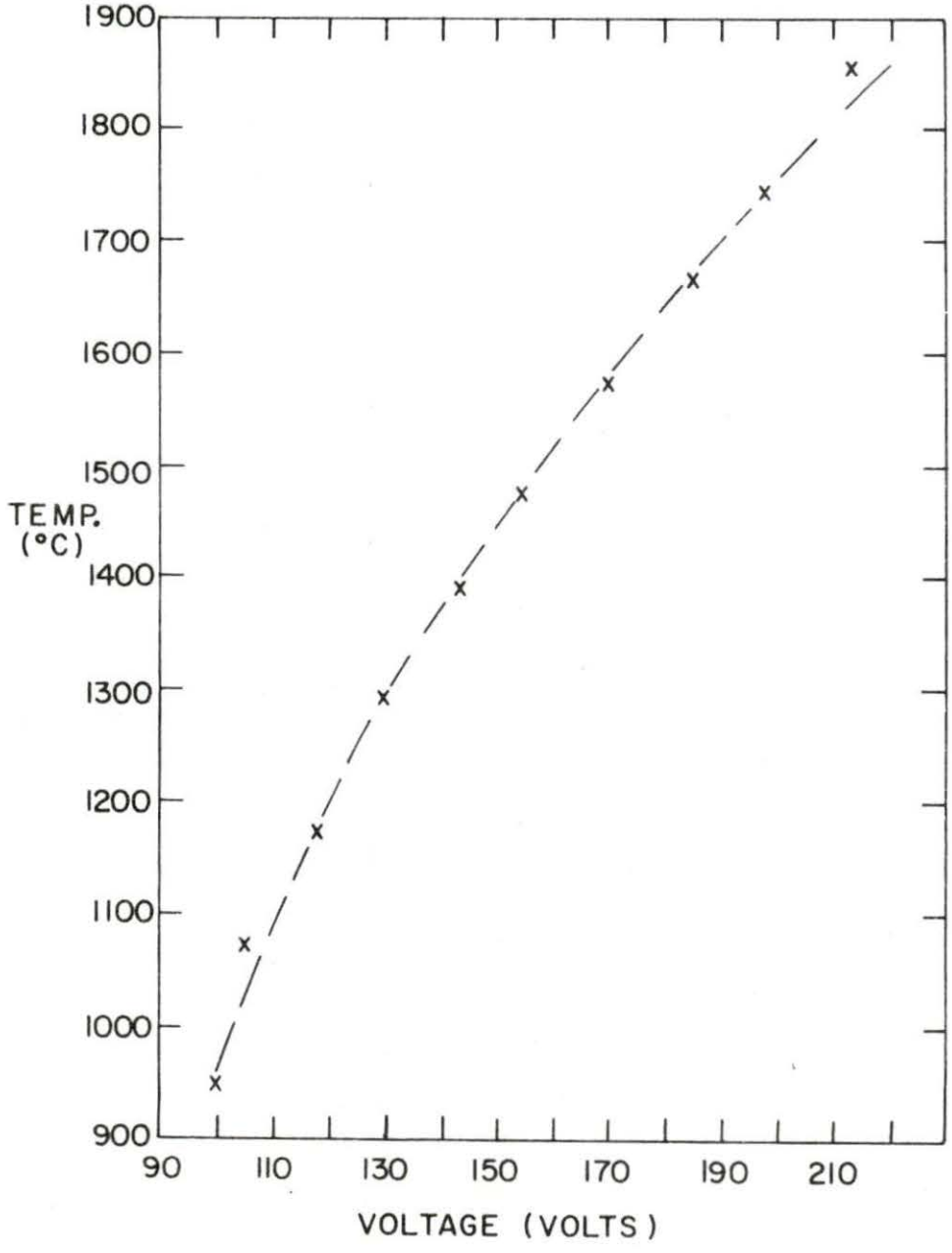

Figure 6. Calibration curve for graphite resistance furnace used in this study

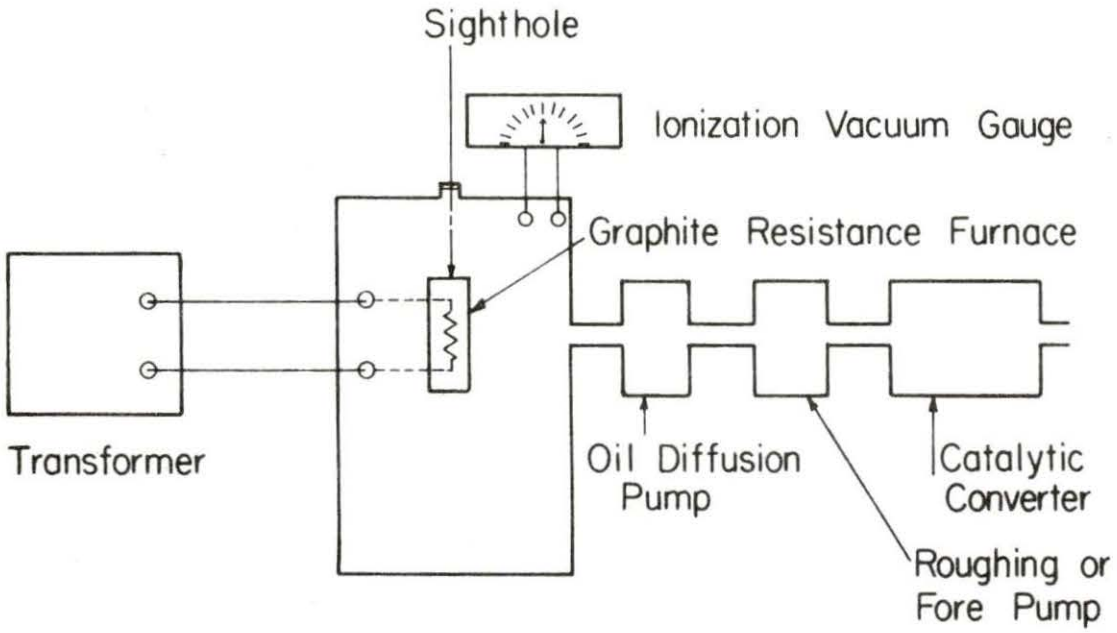

Figure 7. A block diagram of the carbothermic reduction system

of 325 mesh powder and >99% purity was obtained from the Asbury Graphite Company. Baker's analytical grade Sn (20 and 30 mesh) 99.9% pure was used as solvent. Tables 3, 4 and 5 list, respectively, the chemical impurities in the graphite, Nd_2O_3 and Gd_2O_3 materials used in this study.

Table 3. Mass spectrometric analysis of the graphite used in this study

Impurity element	Concentration ppm at.
B	<0.001
Na	<0.002
Al	0.018
Si	0.094
S	0.507
Ca	0.063
Ti	0.028
V	<0.004
Cr	<0.004
Mn	<0.005
Fe	0.931
Ni	<0.005
Cu	<0.005
Zn	<0.005
Mo	0.008
Ba	<0.011
Pb	0.017

Table 4. Mass spectrometric analysis of the Nd_2O_3 used in this study

Impurity element	Concentration ppm at.
B	<0.01
Na	2.27
Mg	<0.5
Al	<8.0
Si	<0.8
S	--
Ca	1.2
Ti	<0.1
V	<0.03
Cr	<0.1
Mn	<0.01
Fe	<1.0
Ni	<0.2
Cu	<0.06
Zn	<0.06
Mo	<0.3
Ba	<0.1
La	<0.8
Ce	0.6
Pr	<0.2
Sm	<0.5
Eu	<0.2
Gd	<2.3
Tb	<4.3
Dy	<1.4
Ho	<0.3
Er	<1.0
Tm	<0.1
Yb	<0.3
Lu	<0.4
Pb	<0.3

Table 5. Mass spectrometric analysis of the Gd_2O_3 used in this study

Impurity element	Concentration ppm at.
B	0.003
Na	<1.3
Al	<0.02
Si	<0.2
S	<0.4
Ca	0.2
Ti	<0.1
V	<0.01
Cr	<0.01
Mn	<0.03
Fe	<1.5
Ni	<0.03
Cu	0.2
Zn	1.4
Mo	<0.3
Ba	<0.04
La	<0.1
Ce	<0.1
Pr	<0.08
Nd	<0.4
Sm	<0.4
Eu	16.3
Tb	<0.9
Dy	<0.4
Ho	<0.1
Er	<2.3
Tm	<0.5
Yb	<1.0
Lu	<1.0
Pb	<0.2

C. Sample Preparation

Samples used in this study were formulated by the following methods:

1. pelletizing rare earth oxides and carbon,
2. pelletizing rare earth oxides, carbon and tin, and
3. jolt packing rare earth oxides, carbon and tin.

1. Pelletizing rare earth oxides and carbon

The first method is the one used by Bakshani et al. for the carbothermic reduction of UO_2 in tin solvent.[11] Neodymium and gadolinium sesquioxides were mixed with carbon by hand in stoichiometric amounts according to the reaction

$$R_2O_3 + 3C \rightarrow 3CO\uparrow + 2R. \qquad (15)$$

The reactants were pressed into cylindrical pellets 3/8" x 1½", under a pressure of 8×10^3 psi, and weighed about 9.5 g. The pelletized reactants were placed in preweighed graphite crucibles. Enough tin was added to completely surround and cover the pellet. Using this method it was found that the molar ratio of Sn to reactants should be at least $5Sn:3C:1R_2O_3$ to prevent gross carbide formation. The resulting assembly was charged to the graphite resistance furnace, and the pressure reduced to 10^{-6} torr before heating to preselected temperatures and times.

2. Pelletizing rare earth oxides, tin and carbon

It was found that the first method did not give reproducible results, as far as carbide formation was concerned. The next step consisted of pelletizing rare earth oxides, carbon and tin in the molar ratio $5Sn:3C:1R_2O_3$ into pellets 3/8" x 1½". The weighed pellets were transferred to graphite crucibles and charged to the graphite resistance furnace,

and the pressure reduced to 10^{-6} torr before heating to preselected temperatures and times.

3. Jolt packing of rare earth oxides, tin and carbon

The pelletizing process was found to be slow and wasteful of reactants. Thus, a faster and more efficient way of sample formulation was sought. The method of jolt packing was found to be faster and less wasteful of materials than pelletizing. Reactants were mixed in the molar ratios $3Sn:3C:1R_2O_3$, $5Sn:3C:1R_2O_3$ and $6Sn:3C:1R_2O_3$. The reactants were transferred to preweighed graphite crucibles and jolted down with a clean graphite rod. The crucible with reactants were reweighed to determine sample mass by difference. The assembly was charged to the furnace and treated as before.

D. Analysis of Samples

1. Metallography, scanning electron microscopy, microprobe analysis and X-ray diffraction

Metallography was done on selected Nd-Sn and Gd-Sn alloys to determine the number of phases in as reduced alloys. The alloys were cut on a diamond tipped saw using acetone as the cutting fluid. They were ground on 600 frit grinding paper and mechanically polished with alumina and isopropanol. All samples had to be stored under argon or vacuum to prevent oxidation by air.

Scanning electron microscopy (SEM) and electron microprobe analysis were performed by Mr. Francis Laabs using an Applied Research Laboratories SEM equipped with a Model EMX electron microprobe. SEM micrographs were obtained using the sample's current. X-ray images or maps were obtained

by scanning the sample's surface with the electron microprobe and feeding the diffracted X-rays into a preamplifier and pulse height selector and onto an observing scope. The X-rays produced spots on the screen of the observing scope; these spots were proportional to the weight fraction of the given element. The weight fractions and ultimately the atom fractions of Sn, Nd and Gd in Nd-Sn and Gd-Sn alloys were determined by the following relation:

$$\frac{\text{X (unknown count rate for a given element)}}{\text{Standard count rate for the same element}} = (\text{wt. fraction})(\text{ZAF}) \qquad (16)$$

where ZAF is a factor that involves the atomic number, fluorescence and mass absorption.[14]

A Debye-Scherer camera was used to obtain X-ray diffraction powder patterns for as-prepared samples.

2. Chemical and gas analyses

The rare earth and tin contents of alloys used in this study were determined by gravimetric analysis and an oxidation-reduction technique, respectively. The total carbon content of alloys was determined by measuring the amount of CO_2 evolved from a burned sample. A number of samples were analyzed for O, N and H by vacuum fusion.

E. Separation of Nd and Gd from Sn Solvent

1. Vacuum distillation

Distillations were done by placing weighed samples of Nd-Sn or Gd-Sn alloys in Ta crucibles surrounded by a Ta susceptor. The susceptor was wrapped with graphite insulating felt to allow higher temperatures to be attained. The assembly was placed inside an inductively heated vacuum

furnace and the pressure reduced to 10^{-6} torr. Power for heating was supplied by a 25 kw Pillar converter. The samples were distilled at temperatures ranging from 1400-1800°C from 3-4.5 hours.

2. Chemical precipitation of tin

Efforts to chemically precipitate tin from the Gd-Sn alloys were done using Ca. Weighed samples of alloys were placed in Ta crucibles along with 10% excess Ca metal. The Ta crucibles were sealed under an argon atmosphere by arc welding. The crucibles were transferred to a Ta susceptor and assembly charged to the inductively heated furnace. Samples were heated at ∿1380°C for 3 hours. The crucibles were removed from furnace after cooling and examined for rare earth metal, Ca and Sn contents and distributions.

IV. RESULTS AND DISCUSSIONS

A. Metallography, Scanning Electron Microscopy, Microprobe Analysis and X-ray Diffraction

Metallographic samples of Nd-Sn and Gd-Sn alloys were extremely difficult to prepare because of rapid oxidation in air. Nd-Sn alloys tended to react in air more readily than Gd-Sn alloys. In addition, it was found that Nd-Sn alloys could not be stored under methanol after polishing because they reacted with it. The best metallographic samples were obtained by mechanical polishing with alumina and isopropanol and placing the sample immediately into jars containing argon. Figures 8 and 9 are 500x photomicrographs of the microstructures commonly found in as-prepared alloys. It appears that Nd-Sn alloys were two phase (Figure 8), i.e., the lighter matrix interdispersed with a gray phase. The number of phases found in Gd-Sn alloys (Figure 9) was somewhat more ambigious than in the case of Nd-Sn alloys. However, it appears that these alloys were three phase, i.e., a lighter matrix interdispersed with a shiny metallic like phase and a black phase. These particular phases were not analyzed by the electron microprobe.

The metallographic samples used to obtain the photomicrographs in Figures 8 and 9 were repolished with alumina and isopropanol and used for scanning electron microscopic (SEM) and microprobe analyses. Scanning electron micrographs of the alloys are shown in Figures 10A and 11A. The long white particle in Figure 10A was identified as carbon using the electron microprobe. Also from Figure 10A, the areas marked a and b were analyzed with the electron microprobe and found to contain 50.89 a/o Sn, 49.11 a/o Nd and 52.86 a/o Sn, 47.14 a/o Nd, respectively. X-ray images

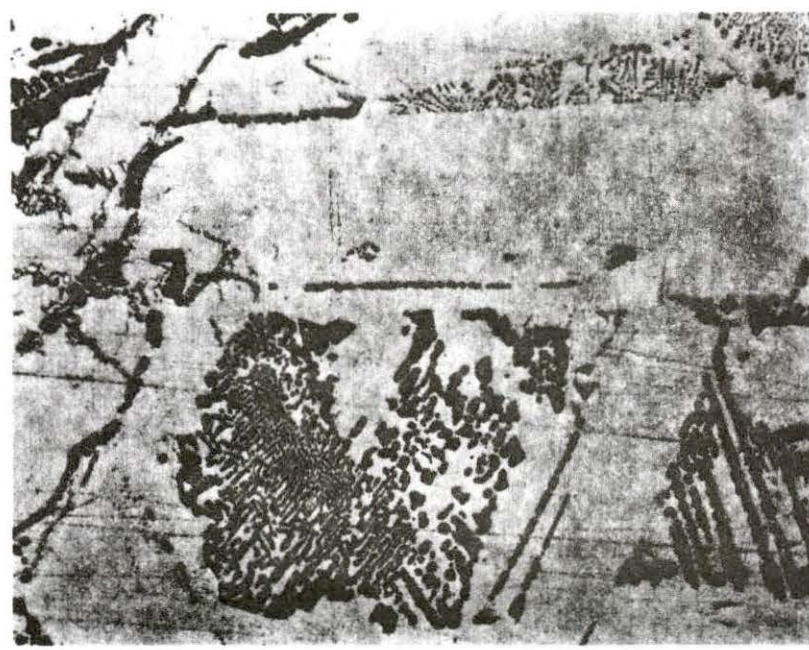

Figure 8. A 500x photomicrograph of the microstructure of an as-prepared Nd-Sn alloy

Figure 9. A 500x photomicrograph of the microstructure of an as-prepared Gd-Sn alloy

Figure 10. A 500x SEM micrograph of the microstructure found in an as-prepared Nd-Sn alloy, and 500x X-ray images formed by the sample current. Areas a and b were analyzed by an electron microprobe

A. 500x SEM micrograph of the microstructure of a Nd-Sn alloy

B. 500x X-ray image of Sn. Light areas are proportional to the weight fraction of Sn

A

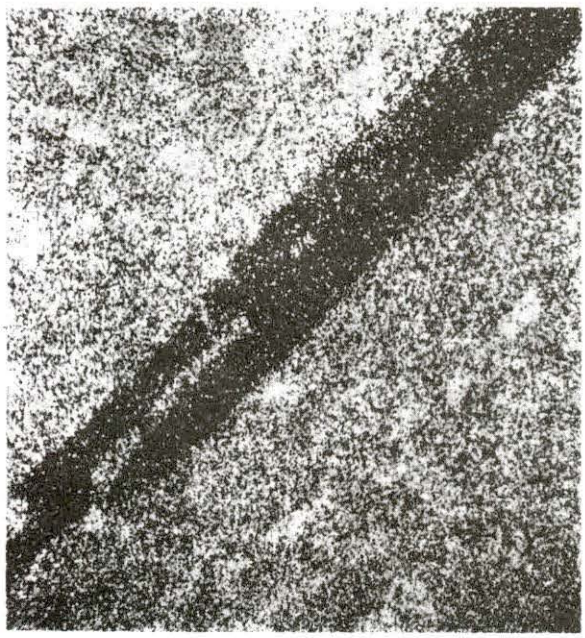

B

Figure 10 (continued)

C. A 500x X-ray image of Nd. The light areas are proportional to the weight fraction of Nd

D. A 500x X-ray image of the carbon particle found in (A). Light spots inside the white particles are proportional to the weight fraction of C

C

D

of the Sn, Nd and C in the Nd-Sn alloy are shown in Figures 10B, C and D. The brightness in these figures are proportional to the weight fraction of Sn, Nd and C. The electron microprobe was focused on arbitrary areas and the composition of Sn and Nd were determined by equation 16 (see p. 27). Using these results, Table 6 was constructed to show the composition of the various phases in the Nd-Sn alloy.

Table 6. Microprobe analysis of Nd-Sn and Gd-Sn alloys used for this study.

Figure number	Area of micrograph	Composition of phases (a/o)		
		Sn	Nd	Gd
10A	a (matrix)	50.89	49.11	—
10A	b (matrix)	52.86	47.14	—
10B	light area	69.94	30.06	—
10B	light area	56.28	43.72	—
10B	light area	59.26	40.74	—
10B	light area	59.68	40.32	—
10C	light area	54.55	45.45	—
10C	light area	53.78	46.22	—
10C	light area	53.34	46.66	—
10C	light area	52.02	47.98	—
11A	a	0.67	—	99.33
11A	b	66.91	—	33.09
11A	c	0.85	—	99.15
11A	d	1.09	—	98.91
11A	e	66.40	—	33.60
11A	f	66.40	—	33.60
11A	g	97.78	—	2.22
11A	h	0.78	—	99.22
11A	i	66.51	—	33.49
11B	light area	66.54	—	33.46
11B	light area	65.17	—	34.83

Figure 11A is a 500x SEM micrograph of a typical as-prepared Gd-Sn alloy used in this investigation. In a similar manner, as in the case of the Nd-Sn alloy, X-ray images of the Sn and Gd from a Gd-Sn alloy was obtained. The brightness of Figures 11B and C are proportional to the weight fraction of Sn and Gd. The electron microprobe was focused on the various areas labeled in Figure 11A and the composition of Sn and Gd were determined by the sample's count rate and equation 16. The microprobe analysis results from the Gd-Sn alloy are summarized in Table 6. From Table 6 it can be seen that there are areas of Figure 11A that are extremely rich in Gd, i.e., areas marked a, c, d and h. These areas or pits were identified as gadolinium oxide by catholuminescence.[14] The composition of the oxide was not determined and was thought to be due to unreacted oxide. Generally, the matrix of the Gd-Sn alloy was fairly uniform. It consisted roughly of ∿67% a/o Sn and 33 a/o Gd.

A Debye-Scherer camera was used to obtain X-ray powder diffraction patterns for as-prepared alloys. It was found that most of the observed lines could be identified as β-Sn or as $NdSn_3$ (a = 4.7060 Å) in the NdSn alloy or as $GdSn_3$ (a = 4.6775 Å) in the Gd-Sn alloy. The lines belonging to β-Sn were identified by computing d-spacings from the observed θ's of Tables 7 and 8 and comparing these to literature values of d-spacings for β-Sn.[15] Similarly, the calculated d-spacings for $NdSn_3$[16] and $GdSn_3$[17] were found to match the non-β-Sn lines in the respective X-ray powder patterns. The results of these studies are summarized in Tables 7 and 8.

Figure 11. A 500x SEM micrograph of the various phases found in a typical Gd-Sn alloy, and 500x X-ray image formed by the sample's current. Small letters a-i are areas analyzed by electron microprobe

A. 500x SEM electron micrograph of the microstructure of a Gd-Sn alloy

B. 500x X-ray image of Sn. The light areas are proportional to the weight fraction of Sn

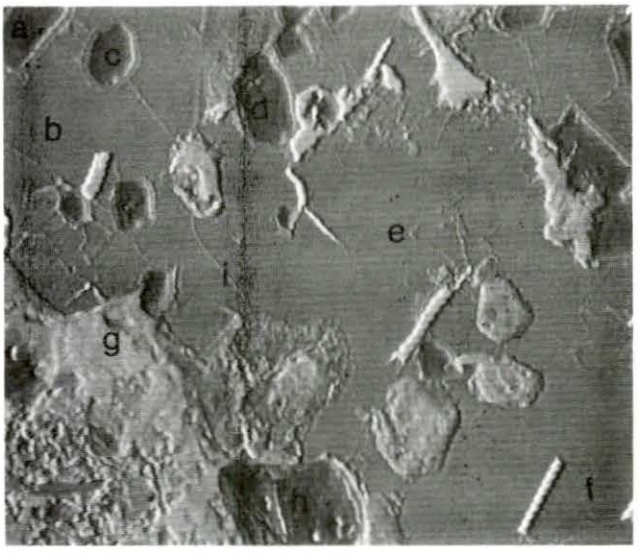

A

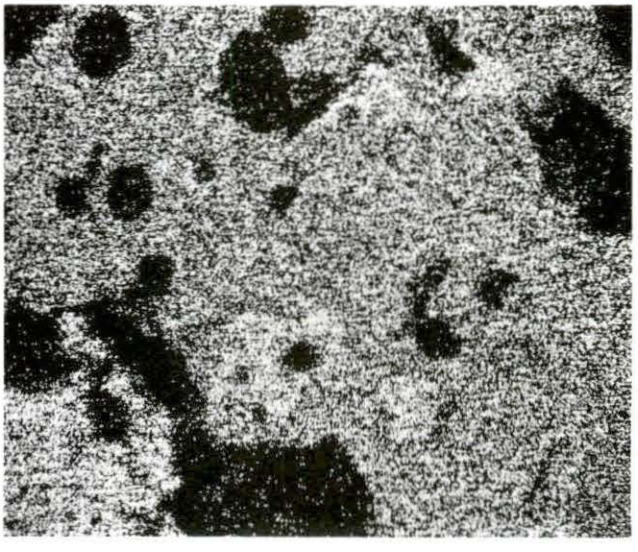

B

Figure 11 (continued)

C. A 500x X-ray image of Gd. The light areas are proportional to the weight fraction of Sn

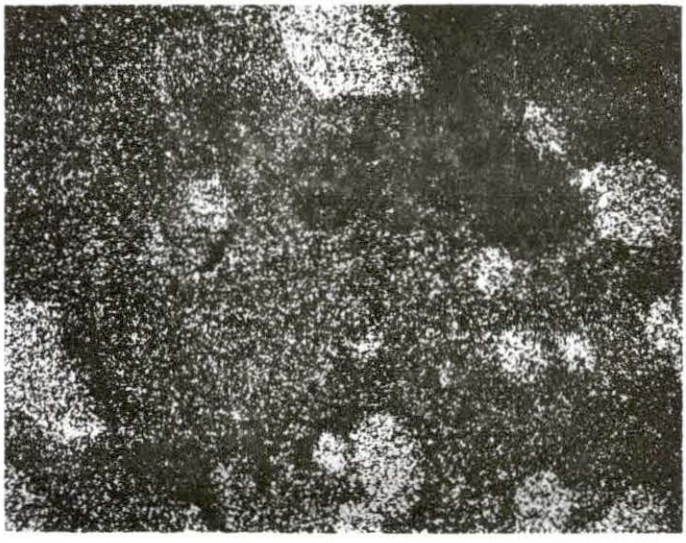

C

Table 7. Observed X-ray data for a Nd-Sn alloy using CuK radiation.

Θ	$Sin^2\Theta$	hkl indices	Phases
15.348	0.0701	200	β-Sn
16.099	0.0770	101	β-Sn
16.550	0.0811	111	$NdSn_3$
22.009	0.1085	200	$NdSn_3$
22.535	0.1469	220	β-Sn
23.537	0.1595	211	β-Sn
27.669	0.2156	220	$NdSn_3$
32.325	0.2707	301	β-Sn
31.976	0.2804	112	β-Sn
32.402	0.2871	311	$NdSn_3$
33.028	0.2971	321	β-Sn
34.631	0.3229	222	$NdSn_3$
36.309	0.3506	?	?
36.684	0.3569	420	β-Sn
79.081	0.941	600,442	$NdSn_3$

Table 8. Observed X-ray data for a Gd-Sn alloy using CuK radiation.

θ	$\sin^2\theta$	hkl indices	Phases
15.450	0.0710	200	β-Sn
16.163	0.0775	101	β-Sn
16.763	0.0832	111	$GdSn_3$
19.338	0.1096	200	$GdSn_3$
22.100	0.1415	220	β-Sn
22.625	0.1480	211	β-Sn
27.825	0.2179	220	$GdSn_3$
32.375	0.2711	112	β-Sn
32.450	0.2879	321	β-Sn
33.225	0.3002	311	$GdSn_3$
35.000	0.3290	222	$GdSn_3$
36.313	0.3507	420	β-Sn
36.700	0.3572	411	β-Sn
39.850	0.4106	?	

B. Chemical and Gas Analyses of Nd-Sn and Gd-Sn Alloys

The times and temperatures necessary to complete the reaction between C and Nd_2O_3 or Gd_2O_3 in a molten Sn matrix were arrived at by trial and error. It was found that pelletizing all reactants or jolt packing them gave the same results as far as could be determined from metallographic and chemical analyses. For the most part, alloys were prepared by jolt packing Sn, C and R_2O_3, since this technique was more convenient. The method used by Bakshani et al. for the preparation of U was ruled out because of extensive carbide formation due to excessive tin losses.(11)

The preparation of Nd-Sn alloys was carried out under a vacuum of 10^{-5} torr and reaction times of 6 and 17 hours and from 1600 to 1700°C, respectively. The reaction time and Sn concentration were held constant for several Nd-Sn samples as the reaction temperature was raised to 1700°C. The purpose of these experiments was to determine the best possible reaction time, temperature and their effects on the amount of retained carbon and oxygen. From Table 9, series A runs, it can be seen that the lowest concentration of retained carbon in Nd-Sn alloys occurred in samples that contained Sn in the molar ratios of 5 and 6 relative to $3C:1Nd_2O_3$. This result was expected since the solubility of C in Sn was almost nil at 1700°C and the amount of Sn was sufficient to tie up the Nd as $NdSn_3$.

Gas analysis of Nd-Sn alloys prepared at 1700°C and a Sn molar ratio of 5 relative to $3C:1Nd_2O_3$ showed about 0.2% C was retained after reaction for 6 hours. This was an indication that the 6 hours reaction time was insufficient. The reaction time was increased to 17 hours and

Table 9. The effects of varying the reaction temperature, the reaction time and tin concentration on the amount of retained carbon and oxygen in Nd-Sn and Gd-Sn alloys.

Sample number	Retained elements (%)				Rare earth content (%)	
	H	C	N	O	Nd	Gd
Series A						
LL-1-26	—	0.264	—	—	44.90	—
LL-1-62	—	0.18	—	—	26.97	—
LL-1-65	—	0.22	—	—	30.80	—
LL-1-68	0.021	—	0.011	0.22	37.21	—
LL-1-103	0.056	1.18	0.01	0.018	43.70	—
LL-1-107	0.005	0.69	—	0.066	37.80	—
Series B						
LL-1-76	0.021	0.56	0.004	0.260	—	36.99
LL-1-80	0.001	0.67	0.005	0.073	—	35.94
LL-1-92	0.11	3.14	0.053	4.30	—	41.82
LL-1-94	0.077	2.44	1.70	2.40	—	40.61
LL-1-96	—	2.13	—	—	—	39.09
LL-1-99	0.081	2.23	2.10	2.20	—	45.89
LL-1-101	0.016	1.82	0.005	0.190	—	50.47
LL-1-109	0.019	1.78	0.0006	0.34	—	42.67

Reaction temperature (^{o}C)	Reaction time (hrs)	Molar ratio of tin to 3C:1R_2O_3
1620	6	5
1960	6	5
1704	6	5
1660	6	5
1700	17	3
1700	17	6
1740	7	5
1760	7	5
1585	17	3
1640	17	3
1680	17	4
1720	17	4
1720	17	3
1760	17	6

the reaction temperature held constant at 1700°C. Since it was determined from previous experiments that if the reaction time was increased past 7 hours, a sufficient amount of Sn was lost by evaporation and would lead to high carbon contents. Thus, the molar Sn ratio was increased to 6 whenever reactions were run at prolonged times (>10 hours) and temperatures in excess of 1700°C. The series A results (Table 9) show the effect of increasing the reaction time to 17 hours on the amount of retained oxygen. The oxygen content dropped by an order of magnitude from 0.22% after 6 hours, to 0.06% after 17 hours. However, the carbon content increased from 0.2% to 0.7%. This result was anticipated, since a longer time at the reaction temperature allowed more diffusion of carbon from the graphite crucible to the sample. In addition, it was found that if the molar ratio of Sn was less than 4, the Nd-Sn alloys obtained at 1700°C contained ∿1.2% retained carbon.

In a similar manner, the best possible reduction conditions for Gd_2O_3 by C were arrived at by trial and error. It was found that the reduction conditions for Gd_2O_3 were more severe than for Nd_2O_3. For example, the series B results in Table 9 show that ∿0.7% C is retained in samples reacted for 7 hours at 1760°C and a molar ratio of 5 Sn to $3C:1Gd_2O_3$. This was roughly 3 times the amount of carbon retained by Nd-Sn alloys under similar conditions. Generally, it was found that the O content was >0.2% and the C content >∿1% for GdSn alloys prepared at temperatures below 1760°C. Figures 12 and 13 show the residual C and O, respectively as a function of reaction temperature. The high C and O contents suggest that the reduction of the Gd_2O_3 is not completed at temperatures below 1760°C. GdSn alloys having the lowest C and O contents were prepared

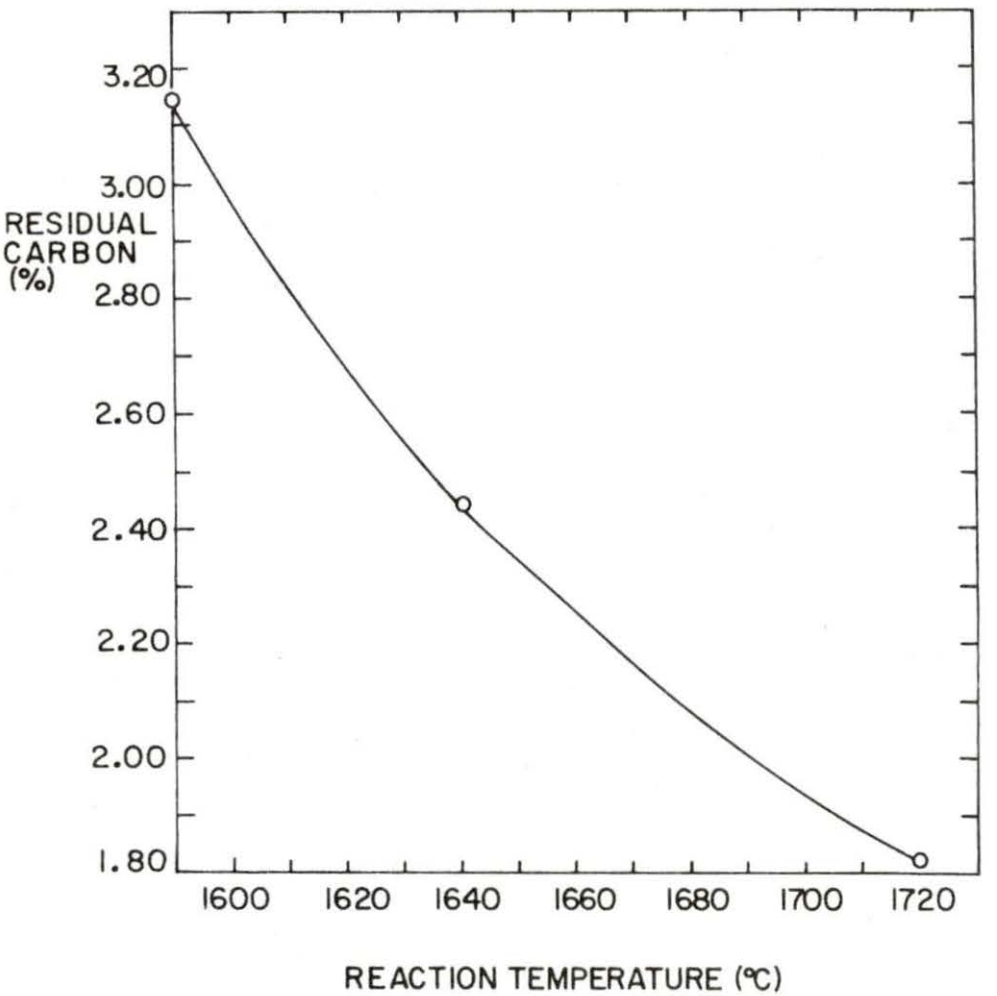

Figure 12. The residual carbon content of Gd-Sn alloys as a function of the reaction temperature. The reactants were in the ratio $3C:3Sn:1Gd_2O_3$. Reaction time was 17 hours

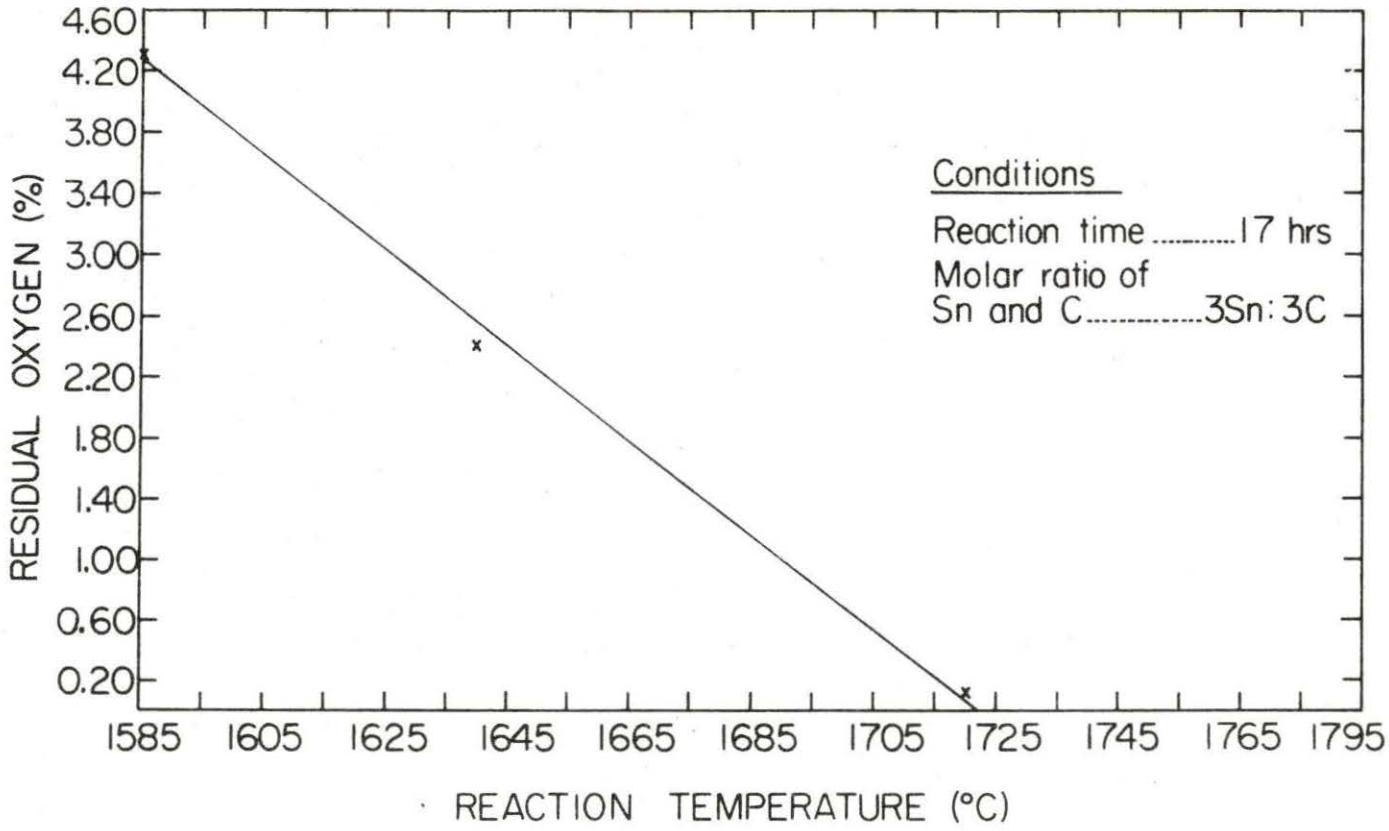

Figure 13. The residual oxygen content of Gd-Sn alloys as a function of the reaction temperature

using a Sn molar ratio of 5 and 7 hours reaction time at 1760°C. The low carbon content was believed to be due to the lack of time for extensive diffusion of carbon from the graphite crucible. The above explanation seemed to be supported by the fact that Gd-Sn alloys as well as Nd-Sn alloys prepared at temperatures in excess of 1720 and 1700°C, respectively, and 17 hours were increasingly contaminated with more than 1.5% carbon.

C. Volatilization of Sn from Nd-Sn and Gd-Sn Alloys

The separation of Sn from Nd and Gd was not accomplished by vacuum distillation over the temperature range 1420-1800°C and a pressure of 10^{-4} torr. Chemical analysis of the distillate from one NdSn alloy showed that 0.2% Nd codistilled with the Sn. The distillant analyzed as 59.9% Sn and 40.1% Nd. Other Nd-Sn alloys showed similar results after vacuum distillation, see Table 10.

Table 10. Chemical analysis of the distillation from Nd-Sn and Gd-Sn alloy.

Sample number	Chemical composition (a/o)			Distillation conditions	
	Sn	Nd	Gd	Time (hrs)	Temperature (°C)
LL-1-29	59.9	40.1	—	$\frac{1}{3}$ followed by	1420 1620
LL-1-63	54.4	45.6	—	3	1760
LL-1-66	51.9	48.1	—	3	1760
LL-1-26	40.9	—	59.1	$\frac{1}{3}$ followed by	1420 1620
LL-1-32	42.3	—	57.7	4.5	1760-1800

A phase diagram for the Nd-Sn system within a range of 0-50 a/o Sn has been determined by Eremenka et al.,[18] see Figure 14. From Table 10 it can be seen that composition of the NdSn alloys used in this study contained slightly more than 50 a/o Sn. Thus, the equilibrium diagram could not be applied directly to these alloys. However, it stood to reason that as more Sn was volatilized the congruent melting phase, Nd_5Sn_3 would result. A comparison of the vapor pressure of pure Sn and Nd at the distillation temperatures (1760°C) showed that it was not likely that Sn could be removed from Nd by vaporization. The vapor pressure of pure Sn at 1760°C was found to be ∿5.7 torr.[13] That of pure Nd at the same temperature was found to be ∿1.7 torr. However, the vapor pressure of the metals will vary across the NdSn system as the activities of the two components vary. But, it should not result in any large relative change in their respective vapor pressures, certainly not enough to allow the Nd and Sn to be separated.

The ease of separation of two components by distillation is measured by the relative volatility, α:[19]

$$\alpha = \frac{\gamma_{Sn} p^{o}_{Sn}}{\gamma_{Nd} p^{o}_{Nd}} \qquad (17)$$

where γ_{Sn} and γ_{Nd} are the activity coefficients of Sn and Nd in solution. p^{o}_{Sn} and p^{o}_{Nd} are the vapor pressures of pure Sn and Nd. For molecular diffusion, Pehlke has rewritten this equation in a more useful form:

$$\alpha = \frac{\gamma_{Sn} p^{o}_{Sn}}{\gamma_{Nd} p^{o}_{Nd}} \quad \frac{\sqrt{M_{Nd}}}{\sqrt{M_{Sn}}} \qquad (18)$$

where M_{Sn} and M_{Nd} are the molar masses of Sn and Nd, respectively. Thus,

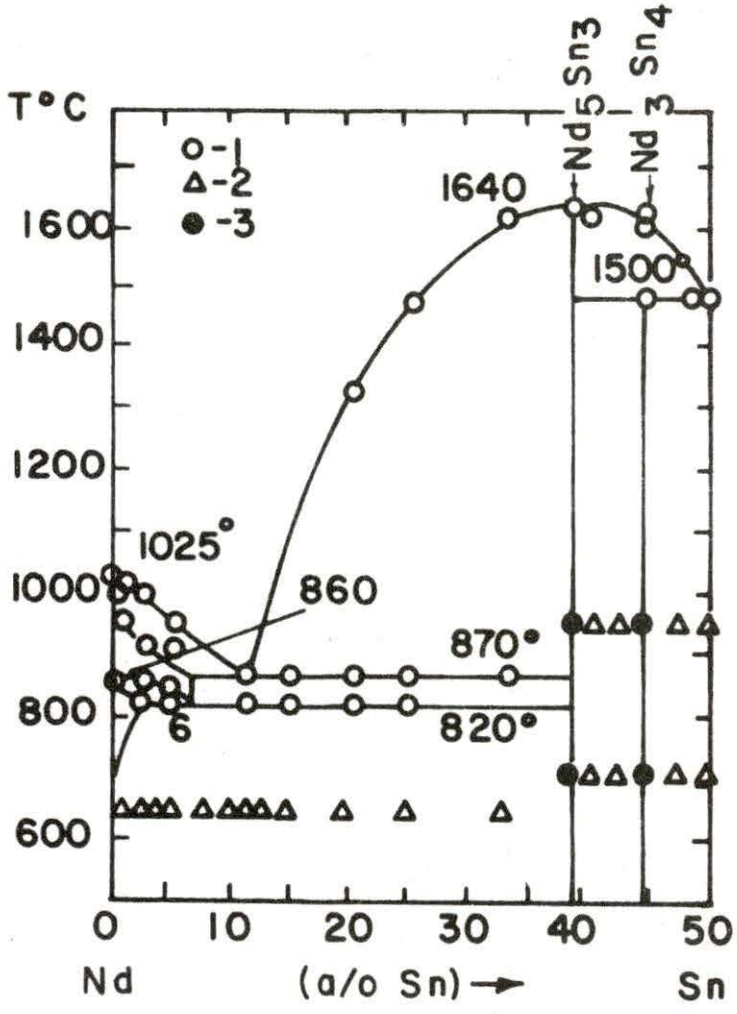

Figure 14. Phase equilibria diagram for the Nd-Sn system within range of 0-50 at % Sn. At 870 ± 10°C L → <β-Nd> + Nd_5Sn_3. At 820 ± 10°C <β-Nd> → <α-Nd> + Nd_5Sn_3. Nd_5Sn_3 melts congruently at 1640 ± 10°C. Nd_3Sn_4 is formed in peritetic reaction at 1500 ± 10°C

if α is unity or close to unity it is not possible to separate Sn and Nd by distillation. And if α is either $\geq 10^3$ or $\leq 10^{-3}$ it should be possible to separate Sn and Nd by distillation.

Even though all of the variables in (18) were not known, namely γ^{o}_{Sn} in Nd, an ideal α was calculated. Although it was realized that γ^{o} for Sn must be less than unity, since Nd has a high affinity for Sn. An α of 1.75 at 1760°C was calculated for the Nd-Sn system. Thus, it should not be possible to separate Sn from Nd by distillation as was observed experimentally, see Table 10.

Somewhat better results were obtained when Gd-Sn alloys were vacuum distilled 1760-1800°C for 4.5 hours. As can be seen from Table 10, the Sn content was reduced to 40.9%. But these results were anticipated since the vapor pressures of Sn and Gd differ by an order of magnitude at 1800°C (5.66 torr vs 0.115 torr).[13] Using the approach of Pehlke as before, an α of equal to 87.6 was calculated for the Gd-Sn system at 1800°C. Again, it was realized that γ of Sn in Gd differed from unity because Gd has a high affinity for Sn. Therefore, theoretically it should be possible to remove more Sn from Gd by distillation under the assumptions made, certainly easier than for Nd-Sn alloys. Results from Table 10 generally tend to support these assumptions, where it can be seen that more Sn was volatilized from Gd than from Nd under the same experimental conditions.

D. Chemical Precipitation of Sn from a Gd-Sn Alloy

A portion of the fourth alloy (LL-1-32) in Table 10 was reacted with Ca to see if it was possible to chemically precipitate Sn as Ca_2Sn. The Ca_2Sn is the most thermodynamically stable of the Ca-Sn compounds.[20]

From Table 10 it was estimated that the fourth Gd-Sn alloy had a composition of Gd_5Sn_3. Enough Ca was added so as to have a 10% excess. The sample was sealed in a Ta crucible under an argon atmosphere by arc welding. The crucible containing the sample was heated inductively for three hours at 1380°C. After reaction, a charred mass was obtained that gave no indication of metallic Gd, as indicated by the absence of magnetic character. The material also contained large flakes of Ta crucible material. No further efforts were made to precipitate Sn chemically with Ca. However, it is felt that a better choice of crucible material such as tungsten, may facilitate the removal of Sn by precipitation with Ca. In addition, it is felt that closer control over the amounts of Ca and stricter temperature regulation may result in the separation of Gd from Sn by precipitation.

V. CONCLUSIONS

The reduction of Nd_2O_3 with carbon in the presence of a Sn solvent was accomplished at 1700°C and a vacuum of 10^{-4}-10^{-5} torr. A reaction time of 17 hours was sufficient to complete the reduction of Nd_2O_3 by C. The molar ratio of Sn to Nd_2O_3 and C was varied from 3 to 6. It was found that a Sn molar ratio of 3 gave the lowest amount of retained O (0.018%) in the final product. However, the retained C content was >1%. Increasing the Sn concentration to $6Sn:3C:1Nd_2O_3$ under the same conditions lowered the retained C content, but increased the O content to 0.06%.

X-ray diffraction powder patterns of Nd-Sn alloys showed $NdSn_3$ of the $AuCu_3$ type structure and excess Sn. Microprobe analysis and SEM of samples showed a Nd-Sn matrix that was approximately 48% Sn and 52% Nd. In addition, there were inclusions in the Nd-Sn matrix that contained carbon. The form of the carbon was not determined.

The separation of Sn from Nd-Sn alloys by vacuum distillation at 1760°C was not accomplished. The removal of Sn from Nd-Sn alloys was not accomplished because the relative volatility, α, was thought to be close to unity. A calculation assuming ideal thermodynamic behavior showed α was 1.75. Thus, it was concluded that the separation of Sn from Nd-Sn alloys could not be done by vacuum distillation.

Reduction of Gd_2O_3 by C in the presence of Sn was found to proceed at 1760°C and a vacuum of 10^{-4}-10^{-5} torr. A reaction time of 17-18 hours under these conditions was necessary to complete the reduction. At temperatures >1760°C the evaporation of Sn was so great that carbide formation could not be prevented. Increasing the molar ratio of Sn to

reactants resulted in more retained O at a given temperature. For example, at a constant reaction temperature of 1720°C and 17 hours reaction time, the retained O contents were 0.19% and 2.20% for Sn molar ratios of 3 and 4, respectively. No correlation was obtained between the retained C constant and molar Sn ratio. This was thought to be due to the fact that samples were prepared in graphite crucibles. However, the carbon content did increase with increasing temperature due to the loss of Sn by evaporation.

X-ray diffraction powder patterns of Gd-Sn alloys showed $GdSn_3$ of the $AuCu_3$ type structure and excess Sn. The Gd-Sn matrix was analyzed by an electron microprobe. The matrix consisted essentially of 60 a/o Sn and 40 a/o Gd. Vacuum distillation of these alloys enriched the Gd content to ∿56 a/o. On further distillation at ∿1800°C, a black magnetic and non-metallic powder of the composition 42.3 a/o Sn and 57.7 a/o Gd remained. Thus, the separation of Sn from Gd-Sn alloys was not accomplished by vacuum distillation. It was thought that the relative volatility, α, of Sn in Gd was close to unity. An ideal thermodynamical calculation at 1800°C for this system gave an α of 87. However, it must be remembered that the activity of Sn in Gd was less than one, since Gd has a high affinity for tin, which would make $\alpha < 87$.

Chemical precipitation of Sn from Gd-Sn alloys with Ca metal was not successful. The product was a sintered mass of reactants and Ta crucible material. However, it was felt that this method deserves further study with a better selection of crucible material, such as W. In addition, it was thought that closer control of reaction temperature and time and

the proper concentration of Ca might lead to the precipitation of Sn from Gd-Sn alloys with Ca metal.

V. REFERENCES

1. Downing, J. H.; Gorski, H. D.; Koerner, E. L., Jr. U.S. Patent 3 104 970, 1963.

2. Beaudry, B. J.; Gschneidner, K. A., Jr. in "Handbook on the Physics and Chemistry of Rare Earths"; Gschneidner, K. A., Jr., Eyring, L., Eds.; North-Holland Publishing Co.: Amsterdam, 1979; Vol. 1, Chapter 2.

3. Bratland, D.; Gschneidner, K. A., Jr. Electrochimica Acta 1980, 25 145.

4. Zwilling, G.; Gschneidner, K. A., Jr. J. Less-Common Metals 1979, 66, 227.

5. Bratland, D.; Gschneidner, K. A., Jr. Acta Chem. Scand.; in press.

6. Zwilling, G.; Gschneidner, K. A., Jr. Z. Metallk.; in press.

7. Wilhelm, H. A.; McCluskey, J. K. J. Metals 1969, 21, 51.

8. Achard, J. C. Rev. Hautes Temper. et Refract. 1966, 3, 281.

9. Kyshtobaeva, G. M.; Smagina, E. I.; Kutsev, V. A. Zhur. Fiz. Khim. 1969, 43, 2400.

10. Anderson, N.; Parlee, N. A. D. J. Vac. Sci. Technical 1976, 13, 527.

11. Bakshani, N.; Parless, N. A. D.; Anderson, R. N. Industrial Research and Development 1979, 21, 121.

12. Kulagina, N. G.; Bayonov, A. P. Zhur. Fiz. Khim. 1974, 48, 466.

13. Hultgren, R.; Desai, P. D.; Hawkins, D. J.; Gleiser, M.; Kelley, K. K.; Wayman, D. D. Selected Values of the Thermodynamic Properties of the Elements, 8th ed.; American Society of Metals: Metals Park, 1978; pp. 201, 344, 482.

14. Laabs, Francis: private cummunication, Ames Laboratory, Iowa State University, Ames, Iowa, July, 1980.

15. Swanson, H. E.; Tatge, E. Journal of Research of National Bureau of Standards 1951, 46, 318.

16. Iandelli, A.; Palezona, A. Atti Accad. Nazl. Lincei Rend. 1960, 40, 623.

17. Harris, I. R.; Rayner, G. V. J. Less-Common Metals 1965, 9, 7-19.

18. Eremenko, V. N.; Khar'Koba, A. M.; Obushenko, I. M. Dopovidi Akad. Nauk Ukr. SSR 1978, 1132.

19. Pehlke, R. D. Unit Processes of Extractive Metallurgy, 3rd ed.; Elsevier North-Holland Publishing Company: New York, 1977; Chapter 5.

20. Kubascheniski, O.; Alcock, C. B. "Metallurgical Thermochemistry"; Pergamon Press: New York, 1979; Vol. XXIV, p. 372.

VI. ACKNOWLEDGEMENTS

I would like to thank Dr. Karl A. Gschneidner, Jr., my major professor, for introducing me to the topic of this thesis, and for his direction and clarification in the interpretation of the information obtained; and to Mr. B. J. Beaudry for his suggestions of experimental methods and construction of the apparatus. I would also like to thank Mr. Harlan Baker for the metallography of the samples, and Mr. Francis Laabs for SEM and microprobe analysis of samples. In addition, I would like to thank Mr. Bernie Evans for the pertinent literature references, and Mr. O. D. McMasters and R. J. Stierman for their help in X-ray diffraction studies. This work was supported by the U.S. Department of Energy, Office of Basic Energy Science, Division of Materials Science.